Statistical properties of a tangentially driven active filament

Matthew S E Peterson, Michael F Hagan and Aparna Baskaran

Martin A. Fisher School of Physics, Brandeis University, Waltham, MA, 02453, United States of America

E-mail: aparna@brandeis.edu

Abstract. Active polymers play a central role in many biological systems, from bacterial flagella to cellular cytoskeletons. Minimal models of semiflexible active filaments have been used to study a variety of interesting phenomena in active systems, such as defect dynamics in active nematics, clustering and laning in motility assays, and conformational properties of chromatin in eukaryotic cells. In this paper, we map a semiflexible polymer to an exactly solvable active Rouse chain, which enables us to analytically compute configurational and dynamical properties of active polymers with arbitrary rigidity. Upon mapping back to the semiflexible filament, we see that the center of mass diffusion coefficient grows linearly with an activity parameter that is renormalized by the polymer persistence length. These results closely agree with numerical data obtained from microscopic simulations.

J. Stat. Mech. (2020) 013216

Contents

1. Introduction

Active systems are characterized by constituents that consume energy to produce directed motion. These systems are inherently out-of-equilibrium, and thus lead to novel steady state behaviors [1, 2]. For example, simple model systems such as active nematics composed of microtubules driven by kinesin motor proteins can continuously create and annihilate topological defects [3–7], and active Brownian particles can aggregate into 'active solids' [8, 9].

Active polymers are a class of active systems that are of considerable interest due to their prevalence in biological systems on multiple length scales, including the flagella of bacterial microswimmers [10, 11], chromatin in eukaryotic cells [12–17], and actin in cellular cytoskeletons [18, 19]. Many studies have focused on the collective dynamics of many such filaments [20–27], and found that activity can lead to behaviors such as formation of clusters [25] and spiral patterns [21, 28, 29].

As in the context of self-propelled particle models [30–36], it is fruitful to understand the properties of isolated active units to provide a framework for understanding the non-equilibrium steady states that emerge in these complex systems. While there are few analytical results available to date [37–43], a number of numerical studies have been undertaken to understand the statistical properties of single active filaments [12, 13, 39, 41, 42, 44–50]. Filaments placed in a bath of active particles can have anomalous dynamic properties, including super- and sub-diffusive motion [12, 13, 41, 42, 44, 45], as well as enhanced diffusion coefficients [39, 46–48]. Activity was also found to lead to the 'softening' of semiflexible filaments, effectively reducing the persistence length, while sufficiently large active forces could lead to chain swelling [40, 51]. Similar results have been found in the case where the active forces are directed along the filament tangent [47, 49], such as in actin or microtubule motility assays.

In this work, we seek to understand the influence of activity on the statistical properties of an isolated semiflexible filament subject to tangential active forces [28, 47, 49], using an analytically tractable model. Note that, neglecting excluded volume interactions, a semiflexible filament with persistence length l_p can be modeled as a Rouse chain with bond length $b \approx 2l_\mathrm{p}$ [52]. Motivated by this mapping, we consider a single active Rouse chain with activity directed along the tangent. We show analytically that activity leads to an enhanced diffusion coefficient that grows *linearly* with the strength of the active force, while the end to end distance of the polymer is *independent* of activity. Mapping the typical Rouse bond length, b, to the persistence length, l_p, we obtain an analytical expression for the diffusion coefficient of an active semiflexible polymer. We compare these predictions to Langevin dynamics simulations of both Rouse chains and semiflexible filaments, and find that our analytical results are able to accurately describe both cases. These results are directly relevant for motility assay experiments [25, 53–56], and elucidate behaviors of active units with internal degrees of freedom.

2. The active Rouse model

A Rouse chain is a simple polymer model wherein we have N beads connected by harmonic bonds. Assuming this chain is in a highly viscous medium with thermal noise, we obtain the familiar Rouse equation of motion for the nth bead [52]

$$\gamma \frac{\partial \mathbf{r}_n}{\partial t} = k(\mathbf{r}_{n+1} + \mathbf{r}_{n-1} - 2\mathbf{r}_n) + \sqrt{2\gamma k_\mathrm{B} T}\boldsymbol{\xi}_n(t), \tag{1}$$

where γ is the damping coefficient, and k the spring constant. Note that the Rouse chain simply collapses to a point in the zero temperature limit. A non-zero temperature is necessary to give the polymer a finite size. The root-mean-square (RMS) bond length is given by $b_0^2 = dk_\mathrm{B} T/k$, where d is the system dimensionality. The thermal noise $\boldsymbol{\xi}_n(t)$ is Gaussian white noise with moments

$$\begin{aligned} \langle \boldsymbol{\xi}_n(t) \rangle &= 0 \quad \text{and} \\ \langle \xi_n^\alpha(t)\xi_m^\beta(t') \rangle &= \delta_{\alpha\beta}\delta_{nm}\delta(t-t'). \end{aligned} \tag{2}$$

3

Equation (1) holds for $n = 2, \ldots, N - 1$. At the ends, we have

$$\gamma \frac{\partial \mathbf{r}_1}{\partial t} = k(\mathbf{r}_2 - \mathbf{r}_1) + \sqrt{2\gamma k_{\mathrm{B}} T}\, \boldsymbol{\xi}_1(t),$$

$$\gamma \frac{\partial \mathbf{r}_N}{\partial t} = k(\mathbf{r}_{N-1} - \mathbf{r}_N) + \sqrt{2\gamma k_{\mathrm{B}} T}\, \boldsymbol{\xi}_N(t).$$

However, we can extend equation (1) to hold for all n provided we allow for 'ghost' beads such that $\mathbf{r}_0 = \mathbf{r}_1$ and $\mathbf{r}_{N+1} = \mathbf{r}_N$. This Rouse model describes an idealized filament in a dry system and has served as an important model for obtaining physical intuition about the statistical properties of polymers [52].

We add tangential activity to this polymer by supposing that the bonds of the polymer impart a force on their attached beads. That is, if the nth bond connects beads n and $n + 1$, then each of those beads experiences some force $\mathbf{A}_n/2$ (so that the total force generated by the bond is $\mathbf{A}_n$). We consider the simple case where

$$\mathbf{A}_n = f_{\mathrm{a}} \times (\mathbf{r}_{n+1} - \mathbf{r}_n),$$

with f_a a constant parameter, in which the equation of motion for an active Rouse chain is

$$\gamma \frac{\partial \mathbf{r}_n}{\partial t} = k(\mathbf{r}_{n+1} + \mathbf{r}_{n-1} - 2\mathbf{r}_n) + f_{\mathrm{a}} \left(\frac{\mathbf{r}_{n+1} - \mathbf{r}_{n-1}}{2} \right) \\ + \sqrt{2\gamma k_{\mathrm{B}} T}\, \boldsymbol{\xi}_n(t). \tag{3}$$

Note that activity could have been implemented by making the beads active, rather than the bonds. But, adding activity to the beads also requires constraining the orientation of the active force, leading to additional complexity (see appendix A). Our implementation of activity is the most tractable for analytical computation, and successfully captures the phenomenology of tangential driving as shown below.

3. Analytical results

Assuming a Rouse chain with a contour length much longer than the bond length b_0, we take the continuous limit of equation (3) to obtain

$$\gamma \frac{\partial \mathbf{r}(n, t)}{\partial t} = k \frac{\partial^2 \mathbf{r}(n, t)}{\partial n^2} + f_{\mathrm{a}} \frac{\partial \mathbf{r}(n, t)}{\partial n} + \sqrt{2\gamma k_{\mathrm{B}} T}\, \boldsymbol{\xi}(n, t) \tag{4}$$

with the boundary conditions

$$\frac{\partial \mathbf{r}(n, t)}{\partial n}\Big|_{n=0,N} = 0, \tag{5}$$

which physically correspond to force-free boundary conditions. We non-dimensionalize this equation by measuring time in units of $d\gamma/k$, distance in units of $b_0 = \sqrt{dk_{\mathrm{B}} T/k}$, and energy in units of $k_{\mathrm{B}} T$. Finally, we let $\alpha = f_{\mathrm{a}} N b_0^2 / 2 d k_{\mathrm{B}} T$ be a measure of activity in our system. As such, α is a measure of the ratio of work performed by the active force to the thermal energy. Our equation of motion now takes the form

$$\frac{\partial \tilde{\mathbf{r}}}{\partial \tilde{t}} = d\frac{\partial^2 \tilde{\mathbf{r}}}{\partial n^2} + \frac{2d\alpha}{N}\frac{\partial \tilde{\mathbf{r}}}{\partial n} + \sqrt{2}\tilde{\boldsymbol{\xi}}(n,\tilde{t}). \tag{6}$$

3.1. Eigenfunction expansion

The general solution of (6) is

$$\mathbf{r}(n,t) = \sum_{p=0}^{\infty} \mathbf{c}_p(t)\phi_p(n) \tag{7}$$

where the $\phi_p(n)$ are the eigenfunctions

$$\phi_p(n) = A_p \mathrm{e}^{-\alpha n/N}\left[\cos\left(\frac{\omega_p n}{N}\right) + \frac{\alpha}{\omega_p}\sin\left(\frac{\omega_p n}{N}\right)\right] \tag{8}$$

where $\omega_p = \pi p + \mathrm{i}\alpha\delta_{p,0}$, and A_p is a normalization factor:

$$A_p^2 = \frac{2}{N}\begin{cases} \alpha\mathrm{e}^{-\alpha}/2\sinh\alpha & p = 0, \\ \pi^2 p^2/(\pi^2 p^2 + \alpha^2) & p > 0. \end{cases} \tag{9}$$

The decaying exponential in these eigenfunctions encodes the breaking of the head-tail symmetry due to the active forces.

The ϕ_p are orthonormal with respect to the weight function $w(n) = \mathrm{e}^{2\alpha n/N}$; that is,

$$\int_0^N \mathrm{d}n w(n)\phi_p(n)\phi_q(n) = \delta_{pq}. \tag{10}$$

We can check that in the limit $\alpha \to 0$, this reduces to the standard cosine series, which is the correct set of eigenfunctions for the passive Rouse chain [52].

Without loss of generality, we assume $\mathbf{r}(n,0) = 0$, so that

$$\mathbf{c}_p(t) = \int_0^t \mathrm{d}s \mathrm{e}^{-\lambda_p^2(t-s)}\boldsymbol{\xi}_p(s), \tag{11}$$

where

$$\lambda_p^2 = \frac{d}{N^2} \times [\pi^2 p^2 + (1 - \delta_{p,0})\alpha^2] \tag{12}$$

and

$$\boldsymbol{\xi}_p(t) = \sqrt{2}\int_0^N \mathrm{d}n w(n)\phi_p(n)\boldsymbol{\xi}(n,t). \tag{13}$$

Unlike a passive Rouse chain, these noise modes are now correlated, so that

$$\langle \xi_p^\alpha(t)\xi_q^\beta(t')\rangle = G_{pq}\delta_{\alpha\beta}\delta(t-t') \tag{14}$$

where

$$G_{pq} = 2\int_0^N \mathrm{d}n w(n)^2 \phi_p(n)\phi_q(n). \tag{15}$$

We now use the eigenfuncton representation of the exact solution to compute the center-of-mass diffusion coefficient and RMS end-to-end distance.

3.2. Diffusion coefficient

The center of mass $\mathbf{X}(t)$ of the chain is given by

$$\mathbf{X}(t) = \frac{1}{N}\int_0^N \mathrm{d}n\mathbf{r}(n,t) = \sum_{p=0}^\infty \mathbf{c}_p(t)\bar{\phi}_p \tag{16}$$

where $\bar{\phi}_p = \int \mathrm{d}n\phi_p(n)/N$ is the average value of ϕ_p over the interval $n \in [0, N]$. From this, we compute the mean square displacement (MSD) as

$$\begin{aligned}
\mathrm{MSD} &= \langle X(t)^2 \rangle \\
&= \sum_{p,q} \bar{\phi}_p\bar{\phi}_q\langle \mathbf{c}_p(t) \cdot \mathbf{c}_q(t)\rangle \\
&= dG_{00}\bar{\phi}_0^2 t + F(t),
\end{aligned} \tag{17}$$

where $F(t)$ is a function that contains only terms that are constant or decay with time (see appendix B). From this, we find the diffusion coefficient to be

$$D(\alpha) = \lim_{t\to\infty}\frac{\mathrm{MSD}}{2dt} = \frac{1}{2}G_{00}\phi_0^2 = D_0\alpha\coth\alpha \tag{18}$$

where $D_0 = 1/N$ is the diffusion coefficient of a passive Rouse chain. Notably, this gives the limiting behaviors

$$D(\alpha) \propto \begin{cases} D_0(1 + \alpha^2/3) & \alpha \ll 1, \\ D_0\alpha & \alpha \gg 1. \end{cases} \tag{19}$$

This result shows that when the active work per bead is small compared to the thermal energy, the diffusion coefficient grows with the square of activity, which is reminiscent of the behavior of an active Brownian particle [57]. However, for $\alpha \gg 1$, i.e. when the active work is large compared to the thermal fluctuations, the diffusion coefficient grows linearly with activity.

At timescales shorter than the rotational relaxation time (discussed in the next section), we expect to see evidence of the active driving through a nonlinear growth in the MSD. After considering the possible effects of inertia, the MSD takes the form

$$\mathrm{MSD}(\delta t) \approx 2dD(\alpha)\delta t + B(\alpha)\delta t^2$$

for $\delta t \ll 1$. Here, the coefficient $B(\alpha)$ describes the ballistic motion of the filament at short times scales. Interestingly, we can show that $B(\alpha)$ actually decays with increasing α. This is discussed further in appendix C.

3.3. Conformational dynamics

There are two relevant parameters that encode the conformational dynamics of the active polymer: the end-to-end length (or the radius of gyration, see appendix D),

which captures its size, and the relaxation time over which correlations in the end-to-end vector decay. We compute each of these quantities here.

The end-to-end vector $\mathbf{L}$ is given by

$$\mathbf{L}(t) = \mathbf{r}(N, t) - \mathbf{r}(0, t) = \sum_{p>0}^{\infty} \mathbf{c}_p(t) \Delta\phi_p, \tag{20}$$

where $\Delta\phi_p = \phi_p(N) - \phi_p(0)$, and the $p = 0$ mode vanishes since $\Delta\phi_0 = 0$. In the long-time limit, we obtain

$$\begin{aligned} \langle L^2 \rangle &= \sum_{p,q>0} \Delta\phi_p \Delta\phi_q \lim_{t\to\infty} \langle \mathbf{c}_p(t) \cdot \mathbf{c}_q(t) \rangle \\ &= d \sum_{p,q>0} G_{pq} \frac{\Delta\phi_p \Delta\phi_q}{\lambda_p^2 + \lambda_q^2}. \end{aligned} \tag{21}$$

While this series representation is the exact result, it converges slowly and does not lend itself to analytical approximation. We compute the sum numerically (see appendix E) and find that

$$\langle L^2 \rangle \approx N. \tag{22}$$

That is, $\langle L^2 \rangle$ is independent of the strength of the active force.

This result can be understood in the context of the microscopic equations of motion given in equation (3) as follows. Since there are no terms that lead to correlations in bond vector orientations in the model, we can envision the polymer as being constructed of uncorrelated active rods. The active forces exerted by these rods cannot change their own lengths, and so the overall length of the polymer is left unchanged. Interestingly, this result does not necessarily hold if the beads are made active instead of the bonds (see appendix A for more details). Further, we expect this result to be modified in the context of the semiflexible polymer where orientational correlations between the bonds can modify the end-to-end length, as discussed in the subsequent sections.

Next, we compute the end-to-end vector autocorrelation function to obtain the rotational relaxation time, τ_R, using the approximation

$$\langle \mathbf{L}(t+\tau) \cdot \mathbf{L}(t) \rangle \propto e^{-\tau/\tau_R} \tag{23}$$

in the $t \to \infty$ limit. Using (20), we see that

$$\begin{aligned} \langle \mathbf{L}(t+\tau) \cdot \mathbf{L}(t) \rangle &= \sum_{p,q>0} \Delta\phi_p \Delta\phi_q \langle \mathbf{c}_p(t+\tau) \cdot \mathbf{c}_q(t) \rangle \\ &= d \sum_{p,q>0} G_{pq} \frac{\Delta\phi_p \Delta\phi_q}{\lambda_p^2 + \lambda_q^2} e^{-\lambda_p^2 \tau}. \end{aligned} \tag{24}$$

As with equation (21), this sum cannot be computed analytically. Assuming it can be approximated by the slowest decaying term ($\propto e^{-\lambda_1^2 t}$), we find the rotational relaxation time to be

$$\tau_R = 1/\lambda_1^2 = \frac{\tau_R^0}{1 + \alpha^2/\pi^2}, \tag{25}$$

where $\tau_R^0 = N^2/\pi^2 d$ is the relaxation time of a passive Rouse filament. Activity therefore reduces the relaxation time. It is worth noting that the approximation in equation (23) is limited in that no individual term of equation (24) dominates. Though equation (25) is the slowest relaxation time, it is not necessarily the dominant one. See appendix F for more details.

3.4. Mapping to a semiflexible filament

Now, we generalize the above results to the case of a semiflexible polymer. Consider a filament as a chain of N beads connected via inextensible bonds of length b_0, with rigidity encoded through the potential

$$H(\{\mathbf{r}_i\}) = \frac{1}{2}\kappa \sum_{i=1}^{N-2} \hat{\mathbf{t}}_i \cdot \hat{\mathbf{t}}_{i+1},$$

where $\mathbf{t}_i = \mathbf{r}_{i+1} - \mathbf{r}_i$ and $\hat{\mathbf{t}}_i = \mathbf{t}_i/|\mathbf{t}_i|$. Activity is added in the same manner as in the case of the Rouse filament. For simplicity, we will neglect excluded volume interactions in these considerations; these will be incorporated in our computational model later.

Suppose our semiflexible filament is constructed of N bonds with typical bond length b_0. We can also view the filament as being constructed of n rigid segments of length $b = 2l_{\mathrm{p}}$. Then using $Nb_0 = nb$, we have

$$\alpha = \frac{f_{\mathrm{a}} N b_0^2}{2d k_{\mathrm{B}} T} = \frac{f_{\mathrm{a}} n b^2}{2d k_{\mathrm{B}} T}\frac{b_0}{b} = \frac{\tilde{\alpha} b_0}{2l_{\mathrm{p}}}.$$

That is, there is an effective activity $\tilde{\alpha}$ for a semiflexible filament that is related to that of a simple Rouse chain through

$$\tilde{\alpha} = 2\alpha l_{\mathrm{p}}/b_0. \tag{26}$$

We hypothesize that if we substitute this renormalized activity into the results for the Rouse chain, they will generalize to the case of an active semiflexible polymer. In particular, equation (18) becomes

$$D(\alpha, \kappa)/D_0 = (2\alpha l_{\mathrm{p}}/b_0) \coth(2\alpha l_{\mathrm{p}}/b_0), \tag{27}$$

which implicitly depends on the stiffness κ through l_{p}. We test this hypothesis using numerical simulations in the next section.

4. Simulation results

In this section, we perform numerical simulations to: (a) validate the continuum approximation of the Rouse chain used to obtain the analytical results, and (b) test the hypothesis of their generalization to semiflexible active polymers with a renormalized activity parameter.
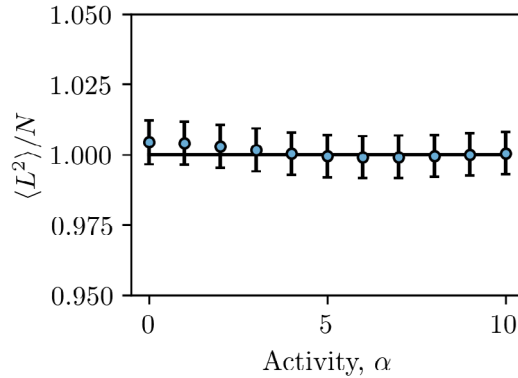
Figure 1. The mean square end-to-end length $\langle L^2 \rangle$ normalized by the number of bonds N is shown as a function of activity α. The horizontal line is the predicted value based on equation (22), the symbols are results from computer simulations, and the error bars show the 95% confidence interval. For all simulation results in this article, we used $N_{\mathrm{atoms}} = 51$ beads.
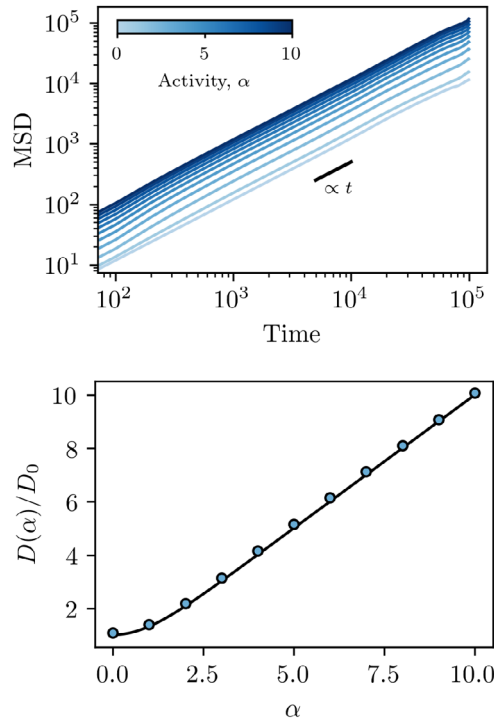
4.1. Active Rouse filaments

To test the continuum limit approximation, we integrate the discrete equations of motion of a Rouse chain, equation (3), for a filament with $N_{\mathrm{atoms}} = 51$ atoms. As before, we non-dimensionalize by measuring energy in units of $k_{\mathrm{B}}T$, time in units of $d\gamma/k$, and length in units of $\sqrt{dk_{\mathrm{B}}T/k}$. Additionally, $f_a = 2d\alpha/N$ where $0 \leqslant \alpha \leqslant 10$ and $N = N_{\mathrm{atoms}} - 1 = 50$ is the number of bonds. We use a time step of $\Delta t = 10^{-3}$ and integrate for a total of 10^8 steps.

We start by considering the steady-state mean square end-to-end length $\langle L^2 \rangle$. For a passive Rouse polymer, we know that $\langle L^2 \rangle = Nb_0^2$, and we expect from equation (22) that this will hold even for an active filament. Indeed, we can see in figure 1 that the polymer size is independent of the strength of the active force. The same result was found when testing chains with shorter lengths as well.

Next, note that based on equation (25), the slowest relaxation time occurs for a passive Rouse chain, for which $\tau_R \approx 10^2$ for the units chosen here. Thus, for lag times $t > \tau_R$, the filament orientations should decorrelate, and so the mean square displacement (MSD) should grow linearly in time. Figure 2 (top) shows the MSD results computed from simulations, which exhibit diffusive motion for times $t \gtrsim 10^2$ for all active force strengths. From these results, we can compute the activity-dependent diffusion coefficient $D(\alpha)$ (figure 2 (bottom)). Here, we observe close agreement between the prediction of equation (18) and the simulation results. In particular, we see the expected linear scaling of the diffusion coefficient with activity for $\alpha > 1$.

4.2. Active semiflexible filaments

To see if the results above are valid beyond the Rouse limit, we consider a more realistic model that incorporates stiff bonds, resistance to bending, and excluded volume interactions. We add these properties by including the potential

Figure 2. Dynamics of active Rouse chains. Top: the mean square displacement (MSD) for Rouse chains as a function of time for various activities, computed from simulation trajectories. For the range of times shown, all of the filaments exhibited purely diffusive motion, with higher activities leading to larger growth in the MSD with time. Bottom: the ratio of the active diffusion coefficient $D(\alpha)$ to the passive diffusion coefficient D_0 for a range of activities. The points are simulation data, and the line is the prediction from equation (18).

$$U(\{\mathbf{r}_n\}) = \sum_{n=1}^{N-1} \frac{1}{2} k(|\mathbf{t}_n| - b_0)^2 + \sum_{n=1}^{N-2} \kappa(1 - \hat{\mathbf{t}}_n \cdot \hat{\mathbf{t}}_{n+1})$$
$$+ \sum_{i \neq j} U_{\text{WCA}}(|\mathbf{r}_j - \mathbf{r}_i|) \tag{28}$$

where $\mathbf{t}_n = \mathbf{r}_{n+1} - \mathbf{r}_n$, b_0 is the preferred bond length, and k and κ set the strength of the bond and angle potentials, respectively. The potential $U_{\text{WCA}}(r)$ is a purely repulsive Weeks–Chandler–Andersen potential [58], defined as

$$U_{\text{WCA}}(r) = \begin{cases} 4\epsilon \left[\left(\frac{\sigma}{r} \right)^{12} - \left(\frac{\sigma}{r} \right)^6 + \frac{1}{4} \right] & r \leqslant 2^{1/6}\sigma, \\ 0 & r > 2^{1/6}\sigma. \end{cases} \tag{29}$$

The equation of motion for the nth bead of the semiflexible polymer is therefore

$$\gamma \frac{\partial \mathbf{r}_n}{\partial t} = -\frac{\partial U}{\partial \mathbf{r}_n} + f_{\text{a}} \left(\frac{\mathbf{r}_{n+1} - \mathbf{r}_{n-1}}{2} \right) + \sqrt{2\gamma k_{\text{B}}T} \boldsymbol{\xi}_n(t). \tag{30}$$

We choose $b_0 = k_{\text{B}}T = 1$, $\sigma = b_0$, $\epsilon = k_{\text{B}}T$, and $k = 200$, and we vary $\kappa \in [20, 100]$.
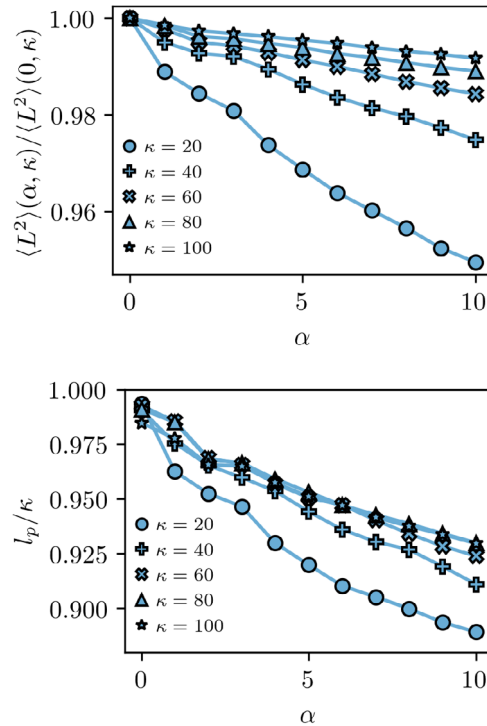
Figure 3. Configurational properties of active semiflexible filaments. Top: the mean-squared end-to-end length computed from simulation trajectories as a function of the activity α for various stiffnesses κ. The results are normalized by those of the passive ($\alpha = 0$) case. In general, we observe $\langle L^2 \rangle$ decaying with α, though this effect is weak over the range of activities tested. Bottom: persistence length l_p normalized by κ as a function of activity. This plot more clearly shows the reduction in l_p with increasing activity, indicating a slight softening of the filament.

We again start by investigating how activity affects the polymer size, in this case looking at both the normalized mean-square end-to-end distance $\langle L^2 \rangle(\alpha, \kappa)/\langle L^2 \rangle(0, \kappa)$ and the persistence length l_p (see figure 3), which is computed by fitting the tangent-tangent correlation function $C_t(m) = \langle \hat{\mathbf{t}}(n + m) \cdot \hat{\mathbf{t}}(n) \rangle$ to the exponential e^{-mb_0/l_p}. In general, we find that activity reduces the size of the polymer, but this effect is weak over the range of activities tested. As such, we see that $l_p \approx \kappa$ for all α, as is expected for a passive semiflexible filament. The decrease in persistence length with activity indicates that activity leads to a slight 'softening' of the filament. This behavior has been studied in-depth in recent work on polymers with directed active forces [28, 47, 49].

We compute the diffusion coefficient $D(\alpha, \kappa)$ for semiflexible polymers and find linear scaling with the parameter αl_p for $\alpha l_p \gtrsim 1$, as shown in figure 4, with $D(\alpha, \kappa) \approx 2\alpha l_p$. To fully test the applicability of equation (27), we performed additional simulations for $\alpha l_p \ll 1$ and found excellent agreement between the measured and predicted values over more than five orders of magnitude.
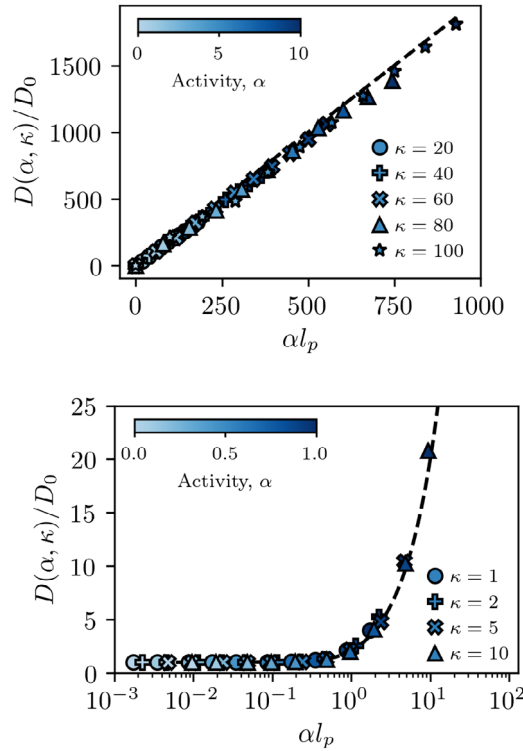
Figure 4. Dynamics of active semiflexible filaments. Top: diffusion coefficients $D(\alpha, \kappa)$ for all simulation parameters as a function of αl_p, the typical net active force exerted on a correlated segment of the filament of length l_p. All of the data lie along the line $D/D_0 \sim 2\alpha l_\mathrm{p}$ (dashed line). Notably, we see the same linear scaling of the diffusion coefficient with activity as with the active Rouse chain (see figure 2). Bottom: diffusion coefficient measured at low αl_p. The dashed line shows equation (27) using the modified activity parameter from equation (26).

5. Summary and discussion

In this paper, we consider a simple model for an active filament in the form of a Rouse chain with an additional force acting along the tangent. By explicitly solving the equation of motion, equation (6), we analytically compute certain configurational and dynamical observables, in particular the MSD, diffusion coefficient, and the end-to-end length as a function of the active force strength. We find that the filament exhibits diffusive motion for times larger than a rotational relaxation timescale, τ_R, which decays rapidly with activity (see equation (25)). This diffusive motion is characterized by an activity-dependent diffusion coefficient that grows linearly with α for $\alpha \gg 1$. This is in contrast to studies on passive filaments in an active bath (see, for example, [39, 41, 45, 48]), which find the diffusion coefficient to grow with the square of the active force strength. In general, studies of polymers with configuration-independent active forces can be well described via an 'effective temperature', whereas configuration-dependent active forces, as studied here, cannot be readily described in this manner.

We verify these analytical results by performing molecular dynamics simulations of an active Rouse chain for a range of active force strengths. As evidenced by figures 1 and 2, we observe excellent agreement between theory and simulation. To test whether the active Rouse model results can be extended to more realistic polymer models, we compare our analytical results to simulations of a semiflexible polymer with excluded volume interactions and stiff bonds. We find that the persistence length is weakly dependent on activity over the range of activities tested (as shown in figure 3), with activity leading to a 'softening' of the filament. This result is consistent with other recent numerical studies on active polymers [28, 47, 49].

Additionally, we find that the diffusion coefficient $D(\alpha, \kappa)$ grows linearly with a renormalized activity parameter, $\tilde{\alpha} = 2\alpha l_{\mathrm{p}}/b_0$. This can be explained by envisioning the semiflexible filament as a Rouse chain with n bonds of length b equal to the Kuhn length $2l_{\mathrm{p}}$, and directly applying the results of equation (18). In principle, this depends non-linearly on activity since the persistence length l_{p} is also activity-dependent. However, for small activities, l_{p} is approximately independent of α, and so we recover the linear scaling of the diffusion coefficient with activity.

Due to the simplicity of this model, it can be readily extended to incorporate richer interactions at the single-filament level. For example, future work could examine how attractive or solvent-mediated interactions affect the behavior of these filaments. These analytical results for the effective activity on an isolated filament can also serve as a starting point for understanding emergent behaviors of dense systems containing many active filaments.

Appendix A. Mean square bond length with active beads

If we imagine a Rouse chain whose beads are the active components, then we must choose a canonical tangent direction for the bead to exert forces in, which must depend on the bond vectors associated to that bead. In particular, we can parameterize the possible tangent vectors $\mathbf{t}_n$ by a parameter ν:

$$\mathbf{t}_n(\nu) = \frac{\nu + 1}{2}(\mathbf{r}_{n+1} - \mathbf{r}_n) - \frac{\nu - 1}{2}(\mathbf{r}_n - \mathbf{r}_{n-1}). \tag{A.1}$$

Consider a Rouse filament consisting of only two beads (and therefore only one bond vector $\mathbf{b} = \mathbf{r}_2 - \mathbf{r}_1$). The equations of motion for these beads takes the simple form

$$\gamma \partial_t \mathbf{r}_1 = k\mathbf{b} + \frac{1}{2}f_{\mathrm{a}}(\nu + 1)\mathbf{b} + \boldsymbol{\xi}_1$$

$$\gamma \partial_t \mathbf{r}_2 = -k\mathbf{b} - \frac{1}{2}f_{\mathrm{a}}(\nu - 1)\mathbf{b} + \boldsymbol{\xi}_2.$$

Subtracting the latter from the former, we obtain an equation of motion for the bond vector:

$$\gamma \partial_t \mathbf{b} = -2(k/\gamma)(1 + \alpha\nu/N)\mathbf{b} + \zeta, \tag{A.2}$$

where we have introduced $\alpha = fN/2k$ and $\zeta = \boldsymbol{\xi}_2 - \boldsymbol{\xi}_1$. This can be readily solved to find

$$\mathbf{b}(t) = \mathbf{b}(0)\mathrm{e}^{-t/\tau} + \int_0^t \mathrm{d}s\,\mathrm{e}^{-(t-s)/\tau}\zeta(s), \tag{A.3}$$

where

$$\tau = \frac{\gamma}{2k(1 + \alpha\nu/N)}. \tag{A.4}$$

Squaring and averaging, we find that in the long time limit

$$b^2 = \lim_{t\to\infty}\langle b(t)^2 \rangle = \frac{2dk_\mathrm{B}T\tau}{\gamma} = \frac{b_0^2}{1 + \alpha\nu/N}, \tag{A.5}$$

where $b_0^2 = dk_\mathrm{B}T/k$ is the mean square bond length of the passive Rouse chain. Thus, we find that activity can lead to compression ($\nu < 0$) or expansion ($\nu > 0$) of the bonds. The bond length is unchanged if $\nu = 0$; in fact, $\nu = 0$ is equivalent to the case where the bonds are the active agents, as used in the main text.

Appendix B. Mean square displacement and the diffusion coefficient

As discussed in the main text, the MSD can be written as

$$\mathrm{MSD} = \sum_{p,q} \bar{\phi}_p \bar{\phi}_q \langle \mathbf{c}_p(t) \cdot \mathbf{c}_q(t) \rangle.$$

Using the definition of $\mathbf{c}_p(t)$ given in equation (11), we have that

$$\langle \mathbf{c}_p(t+\tau) \cdot \mathbf{c}_q(t) \rangle$$
$$= dG_{pq} \times \begin{cases} t & p = q = 0 \\ \mathrm{e}^{-\lambda_p^2\tau}\frac{1 - \mathrm{e}^{-(\lambda_p^2 + \lambda_q^2)t}}{\lambda_p^2 + \lambda_q^2} & \text{otherwise} \end{cases}. \tag{B.1}$$

Thus, for $\tau = 0$, this correlation function approaches a constant if either $p > 0$ or $q > 0$. The only term that grows without bound is the $p = q = 0$ term. The other terms can be collected into the function $F(t)$ as used in equation (17). In particular, we have that

$$\lim_{t\to\infty} \frac{\langle \mathbf{c}_p(t) \cdot \mathbf{c}_q(t) \rangle}{t} = \delta_{p,0}\delta_{q,0} \tag{B.2}$$

which we use to compute the diffusion coefficient as in equation (18).

Appendix C. Effect of inertia

The equation of motion for an active Rouse chain with inertia (in the continuum limit) would be

$$m\frac{\partial^2 \mathbf{r}}{\partial t^2} + \gamma\frac{\partial \mathbf{r}}{\partial t} = k\frac{\partial^2 \mathbf{r}}{\partial n^2} + f_a\frac{\partial \mathbf{r}}{\partial n} + \sqrt{2\gamma k_\mathrm{B}T}\boldsymbol{\xi}(n,t).$$

We can non-dimensionalize this in the same manner as in the main text, measuring time in units of $d\gamma/k$, distance in units of $b_0 = \sqrt{dk_\mathrm{B}T/k}$, and energy in units of $k_\mathrm{B}T$. Defining $\alpha = f_a N b_0^2/2dk_\mathrm{B}T$, we find

$$\tau\frac{\partial^2 \mathbf{r}}{\partial t^2} + \frac{\partial \mathbf{r}}{\partial t} = d\frac{\partial^2 \mathbf{r}}{\partial n^2} + \frac{2d\alpha}{N}\frac{\partial \mathbf{r}}{\partial n} + \sqrt{2}\boldsymbol{\xi}(n,t),$$

where $\tau = mk/d\gamma^2$ is an inertial timescale. As before, we can write the solutions in terms of the eigenfunctions $\phi_p(n)$ as

$$\mathbf{r}(n,t) = \sum_{p=0}^{\infty} \mathbf{c}_p(t)\phi_p(n).$$

The coefficients $\mathbf{c}_p(t)$ now takes the form

$$\mathbf{c}_p(t) = \int_0^t \mathrm{d}s\, H_p(t-s)\boldsymbol{\xi}_p(s),$$

where

$$H_p(t) = \mathrm{e}^{-t/2\tau} \times \frac{2\sinh(z_p t/2\tau)}{z_p},$$

$z_p = \sqrt{1 - 4\lambda_p^2\tau}$, and $\lambda_p^2 = (d/N^2)[\pi^2 p^2 + (1 - \delta_{p,0})\alpha^2]$, as in the main text. Note that for $4\lambda_p^2\tau > 1$, z_p becomes imaginary and oscillatory behavior sets in. This is in contrast to the results found in the overdamped limit, where no oscillatory motion is present.

We can compute

$$\lim_{t \to \infty}\langle \mathbf{c}_p(t + \Delta) \cdot \mathbf{c}_q(t)\rangle$$
$$= dG_{pq} \times \begin{cases} t & p = q = 0 \\ F_{pq}(\Delta) & \text{otherwise} \end{cases} \tag{C.1}$$

where

$$F_{pq}(\Delta) = 8\tau \mathrm{e}^{-\Delta/2\tau}\left\{\frac{(z_p^2 - z_q^2 + 4)\sinh(z_p\Delta/2\tau) + 4z_p\cosh(z_p\Delta/2\tau)}{z_p(4 - (z_p - z_q)^2)(4 - (z_p + z_q)^2)}\right\}. \tag{C.2}$$

We therefore see that, in the long time limit, the $p = q = 0$ term is again the only term that contributes to the MSD, and so the addition of inertia does not affect the diffusive behavior of an active Rouse chain.

We can determine the effect of the active driving at short times by computing

$$\mathrm{MSD}(\Delta) = \lim_{t \to \infty} \langle (\mathbf{X}(t + \Delta) - \mathbf{X}(t))^2 \rangle$$
$$= dG_{00}\phi_0^2 \Delta - \sideset{}{'}\sum_{p,q} [\, f_{pq}(\Delta) + f_{qp}(\Delta)],$$

(C.3)

where $f_{pq}(\Delta) = F_{pq}(\Delta) - F_{pq}(0)$, and primed sums indicate summing over all terms except the $p = q = 0$ term. To second order, we have

$$f_{pq}(\Delta) \approx \frac{2}{\tau} \times \frac{(2\Delta\tau + \Delta^2)(z_p^2 - z_q^2) - 2\Delta^2}{(4 - (z_p - z_q)^2)(4 - (z_p + z_q)^2)}.$$

Noting the terms that are asymmetric in p and q, we can write

$$f_{pq}(\Delta) + f_{qp}(\Delta) = -\Delta^2 b_{pq}$$

where

$$b_{pq} = \frac{8/\tau}{(4 - (z_p - z_q)^2)(4 - (z_p + z_q)^2)}$$
$$= \frac{1}{2\tau} \times \frac{1}{\tau^2(\lambda_p^2 - \lambda_q^2)^2 + 2\tau(\lambda_p^2 + \lambda_q^2)},$$

(C.4)

where in the second line we have used the definition of z_p to rewrite the expression in terms of λ_p. Defining

$$B(\alpha) = \sideset{}{'}\sum_{p,q} b_{pq},$$

(C.5)

we can write the short-time MSD as

$$\mathrm{MSD}(\Delta) \approx 2dD(\alpha)\Delta + B(\alpha)\Delta^2,$$

(C.6)

where $D(\alpha)$ is the diffusion coefficient from equation (18) and $B(\alpha)$ is an activity-dependent coefficient describing the ballistic motion of the system at short times. It's not clear if the sum in equation (C.5) can be computed analytically; however, from the structure of the terms in equation (C.4) we can see that increasing activity *reduces* the value of $B(\alpha)$.

Appendix D. Radius of gyration

In addition to the mean-squared end-to-end distance, $\langle L^2 \rangle$, the radius of gyration, R_g, is a common descriptor of polymer conformations measured in experiments. It is calculated as

$$R_\mathrm{g}^2 = \frac{1}{N} \int_0^N \mathrm{d}n (\mathbf{r}(n,t) - \mathbf{X}(t))^2$$
$$= d \sum_{p,q>0} \frac{G_{pq}}{\lambda_p^2 + \lambda_q^2} \left[\frac{1}{N} \int_0^N \phi_p(n)\phi_q(n) - \bar{\phi}_p \bar{\phi}_q \right].$$

(D.1)
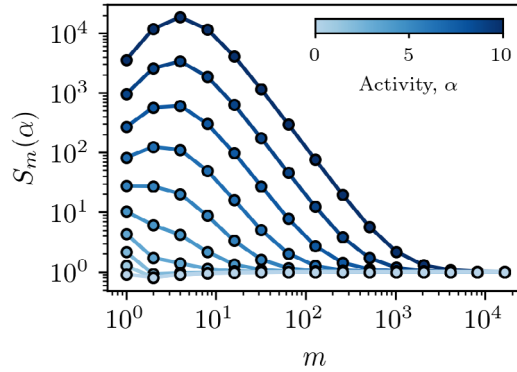
Figure E1. Numerical evaluation of equation (E.3) for various values of the activity parameter α as a function of the number of terms in the sum, m. The sum converges to 1 for all tested activities, for sufficiently large m, with more terms required for larger α values.

As with equation (21), this sum is not amenable to analytic computation, and must be numerically summed. We find that R_{g} is also independent of activity, and converges slowly to

$$R_{\mathrm{g}}^2 \approx N/12, \tag{D.2}$$

which is the same as that of the passive Rouse chain.

Appendix E. Mean square end-to-end distance computation

We claim that equation (21) converges such that equation (22) holds. Here, we give numerical evidence of our claim. Note that, after evaluating equation (15), we can explicitly write the sum as

$$\langle L^2 \rangle / N = \sum_{p,q>0} s_{p,q}, \tag{E.1}$$

where

$$s_{p,q} = 16\pi^4 \alpha \times \frac{p^2 q^2 [(-1)^p \mathrm{e}^{-\alpha} - 1][(-1)^q \mathrm{e}^{-\alpha} - 1][(-1)^{p+q} \mathrm{e}^{2\alpha} - 1]}{(\pi^2 p^2 + \alpha^2)(\pi^2 q^2 + \alpha^2)(\pi^2 (p+q)^2 + 4\alpha^2)(\pi^2 (p-q)^2 + 4\alpha^2)}. \tag{E.2}$$
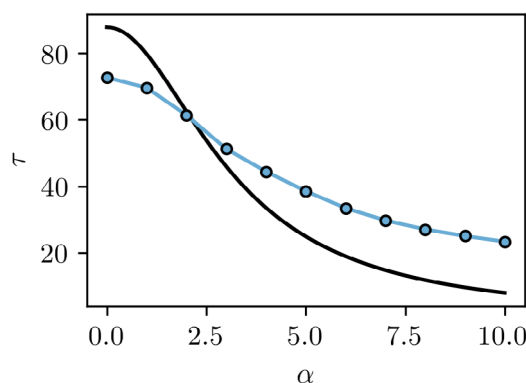
We define the partial sum $S_m(\alpha)$ as

$$S_m(\alpha) = \sum_{p=1}^{m} \sum_{q=1}^{m} s_{p,q} \tag{E.3}$$

so that

$$\langle L^2 \rangle / N = \lim_{m \to \infty} S_m(\alpha). \tag{E.4}$$

In figure E1, we plot $S_m(\alpha)$ against m for a few values of α. In all cases, we see that $S_m(\alpha) \to 1$ as m increases, though for $\alpha > 1$ the partial sum can grow rapidly before decaying, in many cases requiring many millions of terms before we begin to see convergence.

Figure F1. Measured relaxation time (blue dots) compared to that predicted from equation (25) (black line). As expected, activity reduces the relaxation time; however, we only observe qualitative agreement between simulation and theory.

Appendix F. Rotational relaxation time

As discussed in the main text, we find that the slowest relaxation time of an active Rouse chain is

$$\tau_R = \frac{N^2}{\pi^2 + \alpha^2}.$$

However, this relaxation is not necessarily tied to the dominant term in the sum for $\langle \mathbf{L}(t + \tau) \cdot \mathbf{L}(t) \rangle$.

We measure the rotational relaxation time in the simulations by computing $C_{\mathbf{L}}(\tau) = \langle \mathbf{L}(t + \tau) \cdot \mathbf{L}(t) \rangle$ and finding the time τ^* at which $C_{\mathbf{L}}(\tau) = 1/e$. Assuming $C_{\mathbf{L}}(\tau) = \exp(-\tau/\tau_R^{\mathrm{eff}})$, we find that $\tau^* = \tau_R^{\mathrm{eff}}$, where τ_R^{eff} is the effective rotational relaxation time as measured from simulations. Comparisons of τ_R and τ_R^{eff} are shown in figure F1.

References

[1] Ramaswamy S 2010 *Annu. Rev. Condens. Matter Phys.* **1** 323
[2] Marchetti M C, Joanny J F, Ramaswamy S, Liverpool T B, Prost J, Rao M and Simha R A 2013 *Rev. Mod. Phys.* **85** 1143
[3] Sanchez T, Chen D T N, DeCamp S J, Heymann M and Dogic Z 2012 *Nature* **491** 431
[4] Giomi L, Bowick M J, Ma X and Marchetti M C 2013 *Phys. Rev. Lett.* **110** 228101
[5] DeCamp S J, Redner G S, Baskaran A, Hagan M F and Dogic Z 2015 *Nat. Mater.* **14** 1110
[6] Doostmohammadi A, Ignés-Mullol J, Yeomans J M and Sagués F 2018 *Nat . Commun.* **9** 3246
[7] Thampi S P, Golestanian R and Yeomans J M 2014 *Europhys. Lett.* **105** 18001
[8] Redner G S, Hagan M F and Baskaran A 2013 *Phys. Rev. Lett.* **110** 055701
[9] Bechinger C, Di Leonardo R, Löwen H, Reichhardt C, Volpe G and Volpe G 2016 *Rev. Mod. Phys.* **88** 045006
[10] Chelakkot R, Gopinath A, Mahadevan L and Hagan M F 2014 *J. R. Soc. Interface* **11** 20130884
[11] Elgeti J, Winkler R G and Gompper G 2015 *Rep. Prog. Phys.* **78** 056601
[12] Bronstein I, Israel Y, Kepten E, Mai S, Shav-Tal Y, Barkai E and Garini Y 2009 *Phys. Rev. Lett.* **103** 018102
[13] Bronshtein I *et al* 2015 *Nat. Commun.* **6** 8044
[14] Cabal G G *et al* 2006 *Nature* **441** 770
[15] Zidovska A, Weitz D A and Mitchison T J 2013 *Proc. Natl Acad. Sci.* **110** 15555
[16] Ganai N, Sengupta S and Menon G I 2014 *Nucl. Acids Res.* **42** 4145

[17] Haddad N, Jost D and Vaillant C 2017 *Chromosome Res.* **25** 35
[18] Brangwynne C P, Koenderink G H, MacKintosh F C and Weitz D A 2008 *Phys. Rev. Lett.* **100** 118104
[19] Mizuno D, Tardin C, Schmidt C F and MacKintosh F C 2007 *Science* **315** 370
[20] Le Goff L, Amblard F and Furst E M 2001 *Phys. Rev. Lett.* **88** 018101
[21] Prathyusha K R, Henkes S and Sknepnek R 2018 *Phys. Rev.* E **97** 022606
[22] Weber C A, Suzuki R, Schaller V, Aranson I S, Bausch A R and Frey E 2015 *Proc. Natl Acad. Sci.* **112** 10703
[23] Humphrey D, Duggan C, Saha D, Smith D and Kās J 2002 *Nature* **416** 413
[24] Sakaue T and Saito T 2017 *Soft Matter* **13** 81
[25] Suzuki R and Bausch A R 2017 *Nat . Commun.* **8** 41
[26] Sokolov A, Aranson I S, Kessler J O and Goldstein R E 2007 *Phys. Rev. Lett.* **98** 158102
[27] Saintillan D, Shelley M J and Zidovska A 2018 *Proc. Natl Acad. Sci.* **115** 11442
[28] Gupta N, Chaudhuri A and Chaudhuri D 2019 *Phys. Rev.* E **99**
[29] Isele-Holder R E, Elgeti J and Gompper G 2015 *Soft Matter* **11** 7181
[30] ten Hagen B, van Teeffelen S and Löwen H 2011 *J. Phys.: Condens. Matter* **23** 194119
[31] Angelani L, Costanzo A and Di Leonardo R 2011 *Europhys. Lett.* **96** 68002
[32] Ai B-Q, Chen Q-Y, He Y-F, Li F-G and Zhong W-R 2013 *Phys. Rev.* E **88** 062129
[33] Fily Y, Baskaran A and Hagan M F 2014 *Soft Matter* **10** 5609
[34] Basu U, Majumdar S N, Rosso A and Schehr G 2018 *Phys. Rev.* E **98** 062121
[35] Dauchot O and Démery V 2019 *Phys. Rev. Lett.* **122** 068002
[36] Kranz W T and Golestanian R 2019 *J. Chem. Phys.* **150** 214111
[37] Liverpool T B 2003 *Phys. Rev.* E **67** 031909
[38] Gao T, Betterton M D, Jhang A-S and Shelley M J 2017 *Phys. Rev. Fluids* **2** 093302
[39] Eisenstecken T, Gompper G and Winkler R 2016 *Polymers* **8** 304
[40] Eisenstecken T, Gompper G and Winkler R G 2017 *J. Chem. Phys.* **146** 154903
[41] Osmanović D and Rabin Y 2017 *Soft Matter* **13** 963
[42] Osmanović D 2018 *J. Chem. Phys.* **149** 164911
[43] De Canio G, Lauga E and Goldstein R E 2017 *J. R. Soc. Interface* **14** 20170491
[44] Weber S C, Theriot J A and Spakowitz A J 2010 *Phys. Rev.* E **82** 011913
[45] Ghosh A and Gov N 2014 *Biophys. J.* **107** 1065
[46] Di Pierro M, Potoyan D A, Wolynes P G and Onuchic J N 2018 *Proc. Natl Acad. Sci.* **115** 7753
[47] Bianco V, Locatelli E and Malgaretti P 2018 *Phys. Rev. Lett.* **121** 217802
[48] Chaki S and Chakrabarti R 2019 *J. Chem. Phys.* **150** 094902
[49] Anand S K and Singh S P 2018 *Phys. Rev.* E **98** 042501
[50] Das S and Cacciuto A 2019 *Phys. Rev. Lett.* **123** 087802
[51] Harder J, Valeriani C and Cacciuto A 2014 *Phys. Rev.* E **90** 062312
[52] Doi M and Edwards S F 2007 *The Theory of Polymer Dynamics* vol 73 (Oxford: Oxford University Press)
[53] Pringle J, Muthukumar A, Tan A, Crankshaw L, Conway L and Ross J L 2013 *J. Phys.: Condens. Matter* **25** 374103
[54] Farhadi L, Rosario C F D, Debold E P, Baskaran A and Ross J L 2018 *Front. Phys.* **6** 75
[55] Sumino Y, Nagai K H, Shitaka Y, Tanaka D, Yoshikawa K, Chaté H and Oiwa K 2012 *Nature* **483** 448
[56] Schaller V, Weber C, Semmrich C, Frey E and Bausch A R 2010 *Nature* **467** 73
[57] Ghosh P K, Li Y, Marchegiani G and Marchesoni F 2015 *J. Chem. Phys.* **143** 211101
[58] Weeks J D, Chandler D and Andersen H C 1971 *J. Chem. Phys.* **54** 5237

J. Stat. Mech. (2020) 013216